IEEE Access
Multidisciplinary ⋮ Rapid Review ⋮ Open Access Journal

Received 10 May 2023, accepted 5 June 2023, date of publication 4 July 2023, date of current version 14 July 2023.

*Digital Object Identifier 10.1109/ACCESS.2023.3292164*

RESEARCH ARTICLE

# Mattress Sensor-Based Respiration Rate Estimation Using Unsupervised Clustering

**KYEONGTAEK OH[1], JEONGMIN KIM[2], CHEUNG SOO SHIN[2], AND SUN K. YOO[1]**

[1]Department of Medical Engineering, Yonsei University College of Medicine, Seodaemun-gu, Seoul 03722, South Korea
[2]Department of Anesthesiology and Pain Medicine, Anesthesia and Pain Research Institute, Yonsei University College of Medicine, Seodaemun-gu, Seoul 03722, South Korea

Corresponding authors: Sun K. Yoo (SUNKYOO@yuhs.ac) and Cheung Soo Shin (CHEUNG56@yuhs.ac)

This work was supported by the Industrial Technology Innovation Program (Development of Emotional Cognitive and Sympathetic AI Service Technology for Remote (Non-Face-to-Face) Learning and Industrial Sites) funded by the Ministry of Trade, Industry and Energy (MOTIE, South Korea) under Grant 20012603.

This work involved human subjects or animals in its research. Approval of all ethical and experimental procedures and protocols was granted by Institutional Research Board of Severance Hospital under Application No. NCT04964245, and performed in line with the Severance Hospital.

**ABSTRACT** This paper presents a novel approach for measuring the human respiration rate utilizing a mattress sensor. The proposed method employs an unsupervised clustering technique in conjunction with a cluster selection algorithm to accurately measure the respiration rate. The pressure exerted on the mattress sensor reflects the volume changes in the upper body during the breathing process, enabling the estimation of the respiration waveform based on the measured pressure variations. Through the clustering method, the measured pressure changes are effectively separated into respiratory-related clusters and noise. Subsequently, the cluster selection algorithm identifies the optimal combination of clusters that best represents the respiration pattern. To evaluate the performance of the proposed method, it was compared against two alternative methods, namely RWD and RAC. The results demonstrate that the proposed method, referred to as RCS, achieved the highest mean Pearson correlation coefficient of 0.88, indicating superior performance compared to the other methods. In contrast, the mean Pearson correlation coefficients for RWD and RAC were determined as 0.61 and 0.76, respectively. Statistical analysis confirmed the significance of the differences among these methods ($p < 0.001$). Furthermore, a regression analysis was conducted to assess the accuracy of the respiration rate measurements. The findings revealed that the proposed method yielded the most precise estimation of the respiratory rate.

**INDEX TERMS** Respiratory rate, pressure sensor, clustering method, non-contact.

## I. INTRODUCTION

As one of the four vital signs that are important indicators of the state and functions of the human body, respiratory signals have a significant effect on the heart rate variability (HRV). They are very important data for monitoring the condition of ischemic heart disease patients and the onset of respiratory disorder syndrome in newborns. In addition, the estimation of respiratory signals is very important in many cases, as sudden respiratory disorders are directly related to life and must be treated within a short time [1].

The associate editor coordinating the review of this manuscript and approving it for publication was Junhua Li.

In order to measure the respiratory signals of patients, different methods using various sensors have been studied. M. Chu et al. proposed a method to estimate the respiratory rate and volume using a wearable strain sensor [2], while F.T. Wang et al. calculated the respiratory rate using impedance plethysmography [3]. N. Molinaro et al. proposed a method to monitor the respiratory rate using silver plated knitted sensors [4]. However, these methods cause inconvenience to wearers because they must wear the sensor directly on them. To alleviate the discomfort of patients, there have been studies of methods to measure breathing remotely using a camera. M. C. Yu presented a method to estimate the respiratory volume by estimating chest movements and to

examine lung disease caused by chest malformation using a depth camera [5]. K. Alicja et al. presented and analyzed the accuracy of a method to estimate the respiratory rate using thermal camera [6]. L. Scalise et al. presented a method to estimate the heart rate and respiration rate using a web camera [7]. In all of the above methods, the subject of the estimation must be placed in front of the camera. Not only is it difficult to position a patient in front of a camera in a real environment, but it is also challenging to install the camera so that it operates effectively when a patient is lying in bed. Not only camera-based methods, but also methods using microwave radar have been studied. Y. S. Lee et al. used microwave Doppler radar to detect and monitor respiration [8]. They also demonstrated the feasibility of Doppler radar in detecting different types of breathing patterns associated with different breathing sequences. J. Lee and S. K. Yoo proposed radar-based respiration monitoring method using harmonic quefrency selection method and showed that respiration could be continuously detected regardless of the position and measurement duration [9]. Czyżewski, A., et al. proposed a microwave radar-based respiration measurement method that can more accurately measure respiration by applying a heuristic algorithm that provides accurate estimates even in the presence of misleading autocorrelation function maxima [10]. The method using microwave radar works well in the presence of clothes or thin blankets, but it may have limitations when the subject uses thick blankets, and the feasibility has not yet been tested in various sleeping positions.

Using a pressure sensor has the advantages of not having to attach a sensor to the patient's body and of being able to place it under the mattress of the bed, eliminating the need for complicated installation procedures. In addition, it has the advantage of not being restricted by the sleeping position or the situation where the subject sleeps with a thick blanket. Several previous studies have used pressure sensors. M. H. Jones et al. estimated the respiratory rate using a pressure sensor array with the fusion method, which elects the group with the highest weighting from the respiratory rate that is estimated by each sensor [11]. The power spectrum peak detection of the Fourier transform was used to estimate the respiratory rate of each sensor. D. I. Townsend et al. used a pressure sensor array and selected valid sensors by determining whether the signal met two criteria, the upper and lower bounds for the moving variance and moving average to estimate the respiratory rate [12]. M. Holtzman et al. also used a pressure sensor with the spectral ratio method, which utilizes the periodicity of the respiratory signal to ensure that the breathing signal is not discerned from movement [13]. J. M. Kortelainen et al. used a multichannel bed pressure sensor and estimated the respiratory rate using the first principle component score of the principle component analysis (PCA) model applied to the bed sensor signal [14]. S. Nizami et al. used pressure-sensitive mats [15] and applied a frequency domain respiration rate estimation algorithm [16]. These studies focused on extracting a representative respiratory frequency from the signals of the sensor or on selecting a sensor from pressure sensor arrays. However, extracting a representative frequency is difficult to do quickly when there is a change in breathing pattern, and selecting a sensor means that the quality of the breathing signal will inevitably deteriorate if the selected sensor is affected by body movement. Moreover, the position and amount of the pressure applied to the sensor varies over time. Therefore, it is important to dynamically segment only the region affected by respiration, rather than to select a sensor.

Clustering is a type of unsupervised learning that finds the cluster that best represents the given data without labeled data. There are several algorithms for clustering a given set of data points. K-means clustering is commonly used by researchers [17]. It presents the advantage of being fast, involving only a small amount of computation, but has the disadvantage of determining the number of clusters in the initial setting, as the clustering result is strongly dependent on the choice of number of centroids [18]. Mean-shift clustering is a non-parametric iterative algorithm that tries to identify dense areas of data points. Unlike k-means, it does not require prior knowledge of the number of centroids. It has the advantage of being ideal for handling clusters of arbitrary shape and number [19]. It iteratively computes the mean shift until it fulfills a certain convergence condition, and is limited by the fixed kernel bandwidth. The limitation of this algorithm is that the value of the bandwidth parameter is unspecified [20]. Gaussian mixture model clustering is a probabilistic model based on a Gaussian distribution [21]. It has more flexibility than the k-means model, as it assumes that the data points are Gaussian distributed. It also presents the advantage of only requiring a small amount of parameters to learn [22]. The disadvantage of this algorithm is that the spatial relationships between the neighboring data points are not taken into account [23]. The density-based spatial clustering of applications with noise (DBSCAN) is a density-based clustered algorithm. It presents several advantages. First, it does not require prior knowledge specification of the number of clusters. Second, unlike the mean-shift algorithm, which classifies outliers onto a cluster, it identifies outliers as noise. Third, it can find arbitrarily shaped clusters [24]. The disadvantage of this algorithm is that it fails when the clusters are of varying density [25]. Among these various clustering methods, we selected the DBSCAN method, since in order to segment the region related to respiration activity in the pressure sensor, it is necessary to distinguish noise from breathing and to separate the pressure distribution that appears in various forms.

In this paper, we propose a method to measure respiration in a position-invariant manner using an unsupervised clustering method combined with a cluster selection algorithm. The aim of this study was to measure respiration signals using a mattress sensor configured as a pressure sensor. To check the feasibility of the proposed method, we estimated the respiration using a mattress sensor and measured it using a respiration belt in the lying position.

We then compared the proposed method with other methods.

The rest of the paper is organized as follows. Section II introduces the characteristics of the pressure sensor used and how to measure breathing using this sensor. In addition, clustering with the cluster selection method and the method for calculating the respiratory signals are described. Section III shows the experimental results and evaluation of the proposed method. In Section IV, the experimental results and feasibility of the proposed method are discussed. Finally, Section V concludes this paper.

## II. METHODS

In this study, a mattress sensor with a 48 × 48 array of pressure sensors was used to measure the respiration in a non-invasive way. Micro Force Sensors (MFS) developed by MiSung Polytech [26] were used as the pressure sensors. Their structure is shown in Fig. (1a). A MFS is composed of two symmetrical materials with a pressure-sensitive layer between them. The contact resistance of the pressure-reducing layer is used to measure the magnitude of the force applied to the pressure sensor. Each sensor can output a resistance value of 1 KΩ – 1 MΩ and can measure pressure from 0 to 100 kg over a surface of 5 × 5 mm. Fig. (1b) shows a pressure sensor in the form of a mattress in a 48 × 48 array. The sensor data was taken in two-dimensional form within a 48 × 48 matrix and the data was sampled from 14 to 15 Hz. Fig. (1c) shows the experimental environment. To show that the respiratory rate can be estimated using a mattress sensor, the mattress sensor was placed under the subject's upper body (in a supine position), and the respiration was estimated while changing the amount of air supplied by a ventilator. To compare the respiration signals, they were simultaneously measured using a respiration belt manufactured by BIOPAC Systems [27].

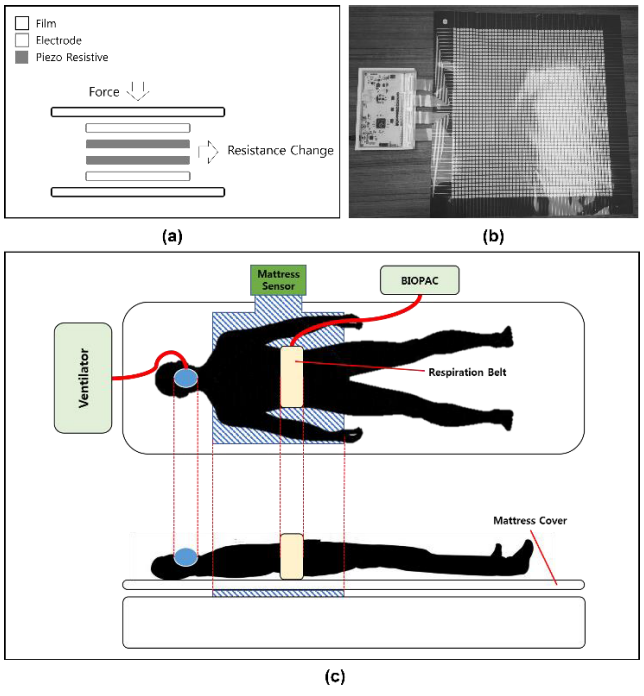


**FIGURE 1.** (a) Structure of the Pressure Sensor, (b) Mattress Sensor, and (c) experimental setup.

Fig. 2 shows the flow chart of the proposed method. When data is acquired from the mattress sensor, the difference is calculated from the sensor data in the time domain. DBSCAN clustering is performed to separate data points where pressure changes appear due to breathing. When clustering is performed, multiple clusters are classified. For each cluster, a respriation waveform is calculated. By FFT conversion, the cluster with the highest peak in the respiration frequency band is selected, and the respiration waveform is finally calculated by inversely transforming the FFT converted respiratrion wavefrom of the selected cluster.

### A. EXPERIMENTAL SETUP

To show the feasibility of the proposed mattress sensor, the respiration signals of a person in a supine position were measured by inserting various input volumes from shallow breathing to heavy breathing using a ventilator. The respiratory activity was recorded independently by a pressure sensor and a respiration belt. Two male subjects (Subject 1: age = 29, BMI = 21.9kg/m$^2$, Subject 2: age = 28, BMI = 23.3kg/m$^2$) without lung disease were recruited for the experiment, and gave their informed consent to participate in the experiment. Before measuring their respiration signals, each subject was trained to breathe with only the air injected by a ventilator. The respiration signals were measured for 2 minutes, 5 times per each subject. All the collected data was used to assess the performance of the proposed method.

### B. MEASURING RESPIRATION WITH A PRESSURE SENSOR

The respiratory process consists of two stages: inhalation and exhalation. During inhalation, as the intercostal muscles and diaphragm contract, the volume of the thoracic cavity and abdomen expands. When a person inhales air, the intercostal muscles contract and expand the volume of the thoracic cavity, while the diaphragm contracts, causing it to descend. When the diaphragm descends to widen the thoracic cavity, the abdominal cavity narrows, causing the abdomen to swell naturally. During exhalation, the contracted intercostal muscles and the diaphragm relax and the extended diaphragm returns to its original dome-shape, causing the volume of the thoracic cavity to contract [28]. This change in volume of the thoracic cavity produces a visible outward movement [29]. In a supine position, when a mattress sensor is placed under the upper body and the person breathes, the change in volume of the thoracic cavity caused by breathing appears as a change in pressure on the mattress sensor.

### C. UNSUPERVISED CLUSTERING

When measuring breathing using a mattress sensor, movements not related to breathing, such as simple body movements that cause pressure changes, compromise the accuracy

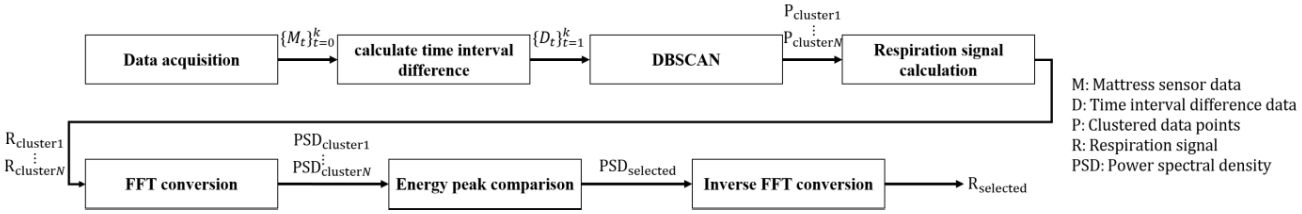


**FIGURE 2.** The flow chart of the proposed method.

of the breathing estimation. Therefore, it is important to isolate the pressure changes caused by breathing in order to measure the respiration signals from the mattress sensor accurately. In addition, depending on the lying posture, the area over which the body contacts the mattress sensor changes and appears random, without a specific form of the area where the pressure related to breathing is transmitted. In this study, we used the density-based spatial clustering of applications with noise (DBSCAN) clustering method [30] proposed by M. Ester to separate the pressure changes related to the respiration. DBSCAN is a density-based clustering algorithm that finds all types of clusters, effectively distinguishes noise, and naturally supports spatial databases [31].

The mathematical principle of the DBSCAN algorithm is as follows. The data set to be processed is defined as $D$, the minimum number of objects in the neighborhood is expressed as MinPts, and the algorithm clustering radius as Eps. If a particular point p in the data set $D$ is the center of a sphere, the data contained within the Eps radius at that point is defined as the Eps neighboring area, which is $N_{Eps}(p) = \{q \in D | dist(p, q) \leq \text{Eps}\}$. Here, $dist(p, q)$ means the Euclidean distance of data points $p$ and $q$. If the number of data points included in the Eps neighborhood of the position of a specific data point $p$ in the data set $D$ is larger than MinPts, it is called a core point. When data points $p$ and $q$ corresponding to data set $D$ are given, if a core point exists and two points are located within the radius of the Eps neighborhood of $p$, then $q$ at $p$ is expressed as direct density-reachable, which is $q \in N_{Eps}(p)$, $\left|N_{Eps}(p)\right| \geq$ MinPts. When data points $p_1, p_2, p_3, \ldots, p_n \in D$ included in data set $D$ are given, and $p_1 = q$ and $p_n = p$, if $p_{i+1}$ are direct density-reachable at $p_i$, $p$ at $q$ is called density-reachable. When data points $p$ and $q$ corresponding to data set $D$ are given, $p$ at $q$ is expressed as density-connected if a particular data point $o \in D$ is density-reachable for $p$ and $q$.

At initiation, the algorithm starts a search of the Eps region adjacent to the data point of interest. If enough data points are around, that is, if more data points than MinPts are given, the cluster is expanded. If not enough data points are given, the points are temporarily classified as noise. These points considered noise may later be found in other Eps neighborhoods, and some of them may be reclassified as part of the cluster. If a data object in the cluster is designated as a core, the Eps neighborhood is also classified as part of the cluster. Therefore, all points in the neighborhood, as well as the core neighborhood, are added to the cluster. This process is repeated until the density-connected cluster is completely determined. Finally, new or unprocessed data is retrieved and classified into clusters or as noise. The algorithm ends when all the data in dataset $D$ has been verified. This process is summarized in Algorithm 1.

**Algorithm 1** DBSCAN Algorithm

**Input:** Dataset D
**Output:** Cluster
DBSCAN(D, MinPts, Eps)
cid ← 0
**for** all the UnChecked P in D do
set P as Checked
N(P) ← SearchNeighbour (P, Eps)
**if** length(N(P)) ≥ MinPts
cid ← cid + 1
ExpandCluster(P, N (P) , cid, MinPts, Eps)
**else**
set P as Noise

ExpandCluster(P, N (P) , cid, MinPts, Eps)
assign P to cluster cid
**for** all the Q in N (P)
**if** Q is UnChecked
set Q as Checked
N(Q) ← SearchNeighbour (Q, Eps)
**if** length(N(Q)) ≥ MinPts
N(P) ← N(P) ∪ N(Q)
**if** Q is unassigned to any cluster
assign Q to cluster cid

### D. RESPIRATION SIGNAL

When using a mattress sensor, respiration signals can be obtained from the change in volume of the thorax. The expansion and contraction caused by breathing are measured as pressure changes by the pressure sensor, and these changes in pressure caused by breathing are measured over time. For the continuous two-dimensional data obtained from the mattress sensor, a median filter with a sample window size of 5 was applied to the time domain to reduce noise. The difference in time was calculated for each data point to measure only the pressure changes caused by breathing. This is represented by (1). The respiration waveform can be calculated differently depending on how the time difference is spaced. In this study,

the respiration waveforms for each time difference were calculated with representative time differences of 1-sample, 15-sample, and 30-sample intervals. The time difference interval was 0.067 seconds for one sample, and 1 second and 2 seconds for 15-sample and 30-sample differences, respectively. Given that the normal breathing rate is 12 to 20 times per minute, the 15-sample time difference corresponds to an approximation of the quarter period of respiration, and the 30-sample difference to an approximation of the half period.

$$D_t = M_t - M_{t-1} \tag{1}$$

In this case, $M_t$ refers to the mattress sensor data obtained at time t, and $D_t$ refers to the two-dimensional data obtained by calculating the difference between the mattress sensor data at time t and the mattress sensor data at time $t-1$. The data $D_t$ is mapped to three-dimensional coordinate points to separate the pressure changes related to breathing. This is as shown in (2).

$$\mathrm{P} = \{\mathrm{x}, \mathrm{y}, D_{t=1,\ldots,k}(\mathrm{x}, \mathrm{y})\} \tag{2}$$

The term P is a set of three-dimensional points, and each three-dimensional coordinate means $D_t(\mathrm{x}, \mathrm{y})$, which calculates the pressure difference over time on the x, y coordinates, with the pressure sensors of the x, y coordinates corresponding to the rows and columns of the mattress sensor. Here, k means the length of the mattress sensor data obtained from the breathing estimation. The DBSCAN algorithm was applied to the three-dimensional point set P to separate the data points related to breathing. This is as shown in (3). To this end, MinPts and Eps were set to 800 and 3, respectively.

$$\mathrm{P}_{resp} = DBSCAN(\mathrm{P}, \mathrm{MinPts}, \mathrm{Eps}) \tag{3}$$

The term $\mathrm{P}_{resp}$ refers to a set of points corresponding to the pressure change related to breathing, as separated by the DBSCAN algorithm. The respiration signal $\mathrm{R}_t$ at a specific time t can be calculated as in (4).

$$R_t = \sum_{\{x,y,t\} \in P_{rest}} D_t(\mathrm{x}, \mathrm{y}) \tag{4}$$

If the length of the mattress sensor data obtained from the breathing estimation is k, the respiration signal measured by each mattress sensor forms a time permutation with length k. In this paper, we define the time permutation of the respiration signal $\{R_t\}_{t=1}^{k}$ as the respiration waveform.

### E. CLUSTER SELECTION

When clustering data related to breathing using the clustering algorithm, a number of clusters are classified. In this paper, we propose a cluster selection method to find the combination of clusters that best represent the respiration among the many classified clusters. The algorithm can be described as follows. A better respiration signal is selected by comparing the respiration signal calculated in the first cluster with the respiration signal calculated in another cluster. Then, each respiration signal is FFT-converted and the respiration signals are compared by selecting the larger value of the energy peaks in the 0.1–1 Hz band corresponding to the respiration frequency in the power spectrum. The clustering algorithm repeats the comparison for as many combinations of multiple clusters that have been separated as respiration, and finally selects the combination of clusters with the highest peak value that is, the combination of clusters with the least noise.

## III. RESULTS

We measured the respiration signals of a person in a supine position by inserting various input volumes from shallow breathing to heavy breathing using a ventilator. In addition, the clustering algorithm was used to calculate the respiration waveform by separating the respiration-related areas. To demonstrate the superiority of our proposed method, we compared the respiratory waveforms of various methods. First, we extracted respiratory waveform without using DBSCAN clustering method (RWD). Second, we extracted respiratory waveform using all the separated clusters using DBSCAN (RAC). Last, we extracted respiratory waveform using clusters which was selected from the clustering selection method (RCS).

### A. RESPIRATION WAVEFORM COMPARISON BETWEEN DIFFERENCE TIME INTERVALS

When calculating the respiration signals using the mattress sensor, the time difference was calculated for each piece of data to measure the pressure change caused by breathing.

The respiration waveform was calculated for time differences of 1 sample, 15 samples (quarter period of normal breathing), and 30 samples (half period of shallow breathing). The results are shown in Fig. 2. When the time interval is a 1-sample difference, when compared with the respiration waveform of the respiration belt, it can be seen that there is a lot of noise together with the respiration signal, and that the respiration pattern is hard to distinguish. When the time interval is a 15-sample difference, the respiration pattern is more clearly distinguishable than in the case of a 1-sample difference. However, the breathing peak is not seen clearly. With a time interval of 30 samples, it was found that the respiration waveform was similar to the respiration waveform of the respiration belt, and the breathing peak was also seen most clearly. When the Pearson correlation coefficient between the respiration waveform of the respiration belt and the respiration waveform calculated from the time intervals of 1-sample, 15-sample, and 30-sample differences was calculated, it was sequentially calculated as 0.24, 0.74, and 0.83. This shows that the respiration waveform at 30 samples is the most similar to that of the respiration belt, as seen in Fig. 3.

### B. RESPIRATION-RELATED REGION SEGMENTATION

The clustering algorithm was applied to separate the noise from the data related to breathing. Fig. 4 shows the clustering results of the clustering algorithm two-dimensionally in 10 experimental cases. In Fig. 4, the x and y axes represent the columns and rows of $48 \times 48$ sensors. Fig. 4 shows that respiration-related clusters are distributed at various locations

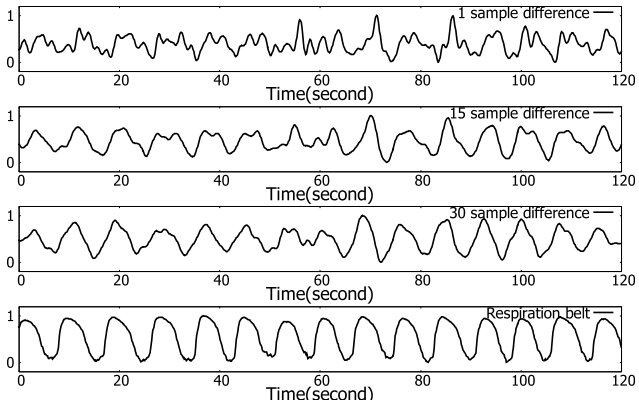


**FIGURE 3.** Respiration waveform comparison between difference time intervals.

in each case. In all cases, however, the respiration-related clusters were found to be mainly distributed in areas with more than 36–48 rows. In Fig. 4, the data classified as noise were excluded from the display. Fig. 5 shows the results of the clustering algorithm in three dimensions. In Fig. 5, each of the x, y, and z axes indicates the values obtained by calculating the difference between the rows and columns of the 48 × 48 sensor array, and between the measured the pressure values and pressure values at 30-sample time intervals. In Fig. 5, it can be seen that a total of three clusters and noise were separated, and that the position of the change in the pressure value is not distributed throughout the 48 × 48 matrix of the pressure sensor, but is clustered between rows 44 and 48.

Fig. 6 shows the respiration waveforms calculated for each cluster and the respiration waveforms of the respiration belt. It presents the values calculated from each cluster and the respiration belt. Among the data classified as respiration-related clusters, cluster 3 was calculated to be the most similar to the respiration waveform of the respiration belt. Next, it was found that cluster 1 was similar to the respiration waveform of the respiration belt, while cluster 2 was the most different from the respiration waveform of the respiration belt. It was hard to find the respiration pattern in the data classified as noise. Therefore, it was found that the noise had been effectively separated by the clustering algorithm. The Pearson correlation coefficients were calculated as 0.68, 0.52, and 0.91, respectively, for each cluster number in ascending order, and as 0.12 for the data classified as noise.

### C. EVALUATION OF RESPIRATION WAVEFORMS

In this paper, the respiration waveforms were evaluated by calculating the Pearson coefficient of correlation between the respiration waveforms measured using the respiration belt and the respiration waveforms calculated in all the experimental cases. Table 1 compared the respiration waveforms extracted from different methods. Table 1 showed that the Pearson correlation coefficient was the lowest when using RWD in all cases, while it was the highest when using RCS.

**TABLE 1.** Evaluation of respiration waveforms generated by different methods.

| Case No. | RWD | RAC | RCS |
|---|---|---|---|
| 1 | 0.37 | 0.58 | 0.84 |
| 2 | 0.72 | 0.84 | 0.92 |
| 3 | 0.12 | 0.62 | 0.75 |
| 4 | 0.86 | 0.87 | 0.88 |
| 5 | 0.78 | 0.83 | 0.90 |
| 6 | 0.33 | 0.57 | 0.84 |
| 7 | 0.71 | 0.83 | 0.91 |
| 8 | 0.83 | 0.84 | 0.92 |
| 9 | 0.66 | 0.77 | 0.86 |
| 10 | 0.71 | 0.79 | 0.95 |
| Mean | 0.61 | 0.76 | 0.88 |
| STD | 0.24 | 0.11 | 0.06 |

* STD: Standard Deviation

Moreover, the means of the Pearson correlation coefficients were 0.61, 0.76, and 0.88, respectively, showing that the lowest mean was found for RWD, while the RCS yielded the highest mean. Fig. 7 shows the linear regression results of the Pearson correlation values for each method for the input volume. In the case of the RWD, the slope and offset of the linear model were 0.299e-4 and 0.323. If the input volume is low, the Pearson correlation coefficient is low, while if the input volume is large, the Pearson correlation coefficient is high. In the case of RAC, the slope and offset of the linear model were 0.162e-4 and 0.601. This is less affected by the input volume than when not using clustering. However, it can be seen that the Pearson correlation coefficients tend to be small with a small input volume and to be large with as large input volume. The slope of the linear model was calculated to be the lowest (0.234e-5) and had the highest offset 0.852 when using RCS. Compared with other methods, it was relatively unaffected by the input volume, and the Pearson correlation coefficient was calculated to be high.

### D. EVALUATION OF RESPIRATION RATE

In this paper, the respiration rate was calculated using the respiration waveforms calculated with each method and was compared with the respiration rate calculated with the respiration belt. Fig. 8 shows the linear regression results for the respiration rate calculated with each method and the respiration rate calculated with the respiration belt. In Fig. 8, RWD exhibits a linear model slope of 0.564 and achieves the lowest coefficient of determination (0.67), indicating the lowest agreement with the respiration rate from the respiration belt. On the other hand, the slope of the linear model of RCS was 1.031. This method achieved the highest coefficient of determination (0.99), showing the highest level of agreement with the respiration rate measured by the respiration belt. Fig. 9 shows the Bland-Altman plots evaluating systematic

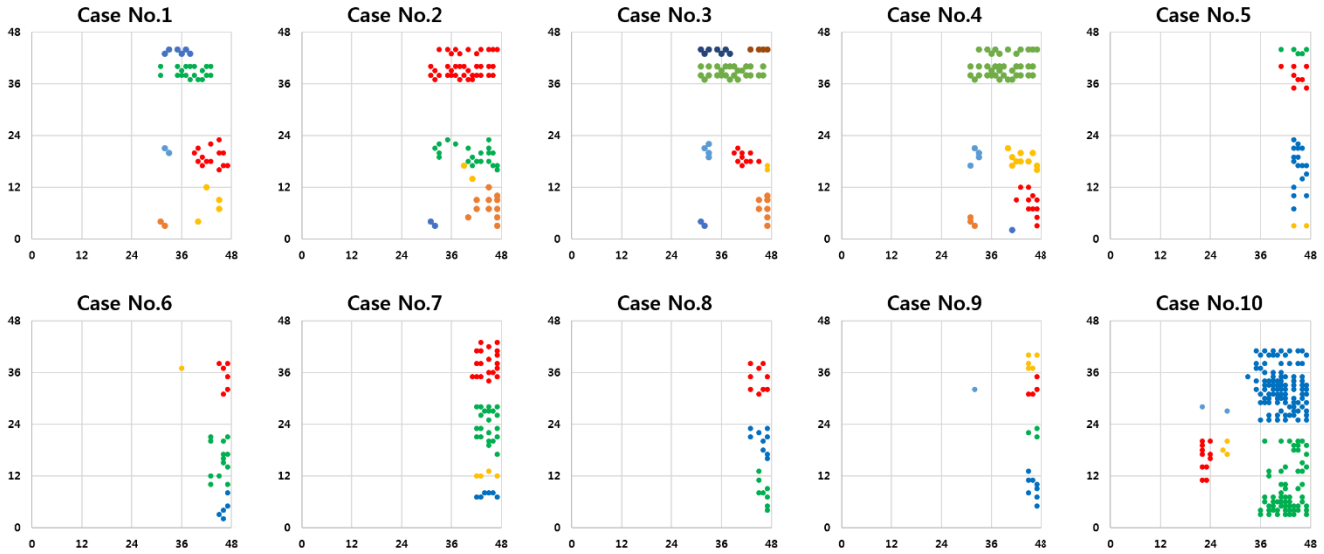


**FIGURE 4.** Distribution of the respiration-related clusters using the clustering algorithm.

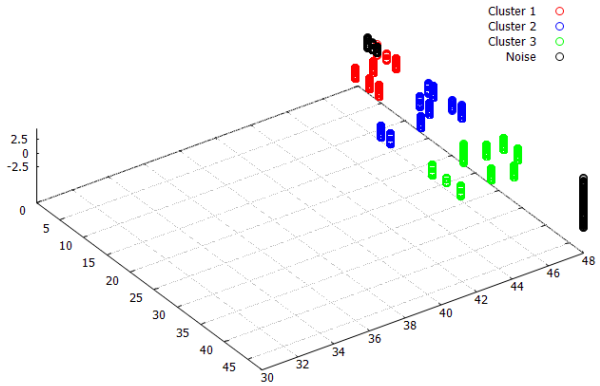


**FIGURE 5.** Respiration-related region segmentation using the clustering algorithm.

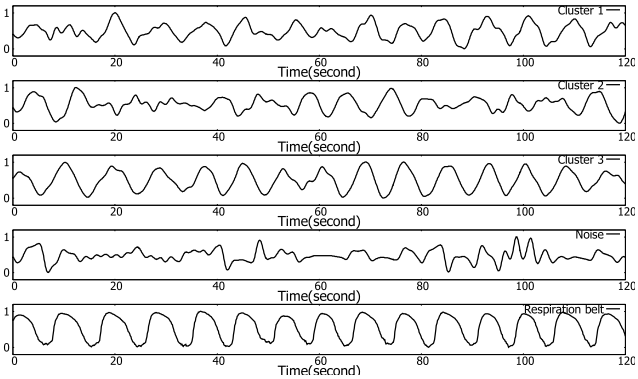


**FIGURE 6.** Respiration waveform comparison between difference clusters.

bias of different methods against ground truth number of breath. The RWD under estimated the number of breath compared to the respiration belt (bias $= -1.50 \pm 3.17$, 95% limits of agreement $= [-7.72, 4.72]$). In the case of RAC, the bias became smaller and had narrower 95% limits of agreement compared to RWD (bias $= -0.60 \pm 1.58$, 95% limits of agreement $= [-3.69, 4.49]$). In the case of RCS, RCS had the smallest bias and narrowest 95% limits of agreement (bias $= -0.10 \pm 0.32$, 95% limits of agreement $= [-0.72, 0.52]$).

## IV. DISCUSSION

In this study, we segmented the breathing-related regions that appeared at various locations when measuring breathing using a mattress sensor and a clustering algorithm. We checked the distribution of clusters in each experimental case. As a result, it was found that respiration-related clusters were distributed in regions of different shapes and sizes in each experiment, and that they were mainly distributed in rows 36–48, at the edges of the sensor. In this region, the corresponding body part is the abdominal area. Therefore, it was found that the pressure sensor mainly detects the volume change of the abdomen caused by respiration.

In our study, we proposed a method to selectively identify the clusters most relevant to respiration among those generated using the DBSCAN algorithm. Consequently, when employing the cluster selection method, the mean Pearson correlation coefficient reached its highest value of 0.88, indicating the ability to accurately calculate the respiration waveform most akin to the reference respiration belt. As illustrated in Table 1, the RWD method, which does not utilize clustering, exhibited considerably low correlations. With mean Pearson correlation coefficients of 0.37, 0.12, and 0.33 for Cases 1, 3, and 6, respectively, the RWD method demonstrated a notable lack of reliability. On the other hand, the RAC method, which exclusively employed the DBSCAN clustering technique, yielded higher accuracy compared to the RWD method. The mean Pearson correlation

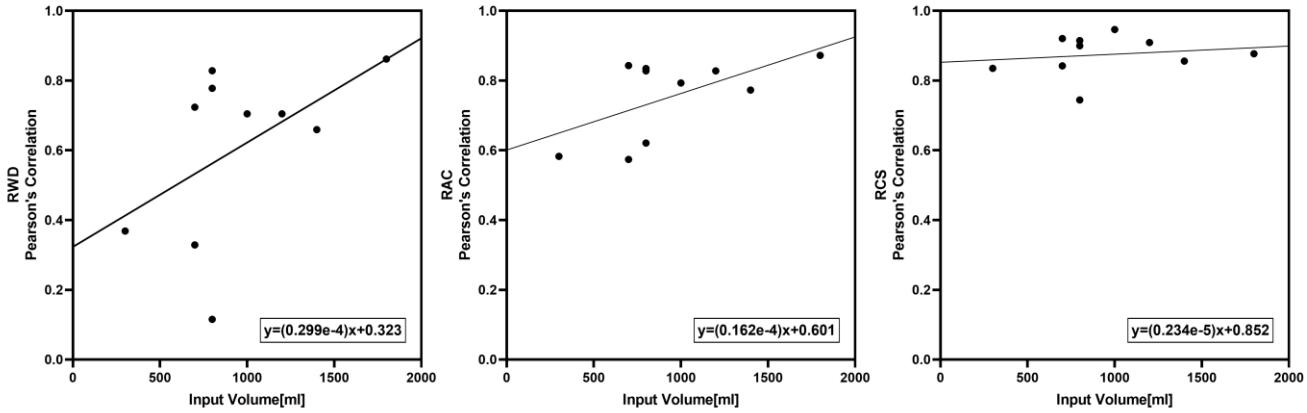


**FIGURE 7.** Pearson correlation comparison of input volume between the different methods.

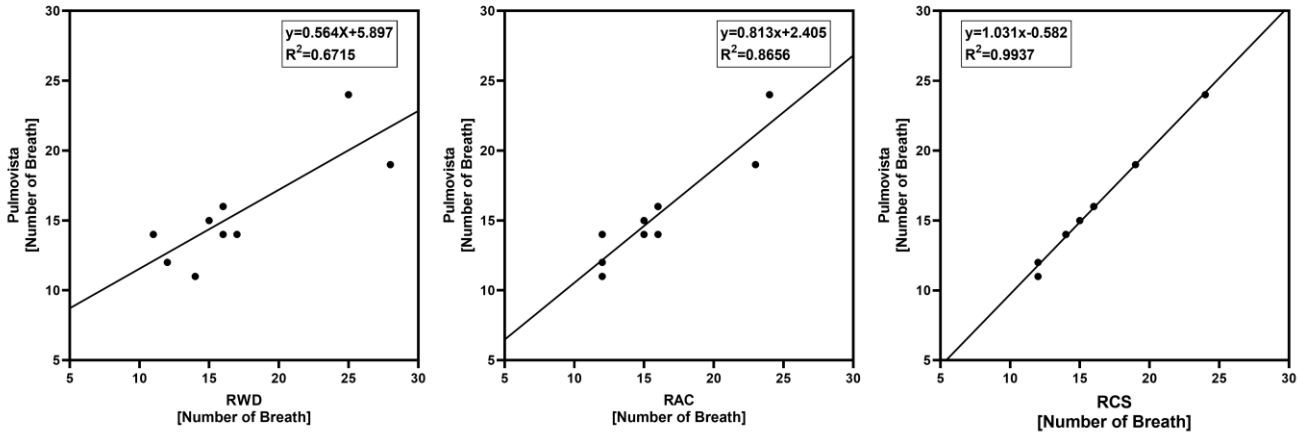


**FIGURE 8.** Respiration rate comparison between the different methods.

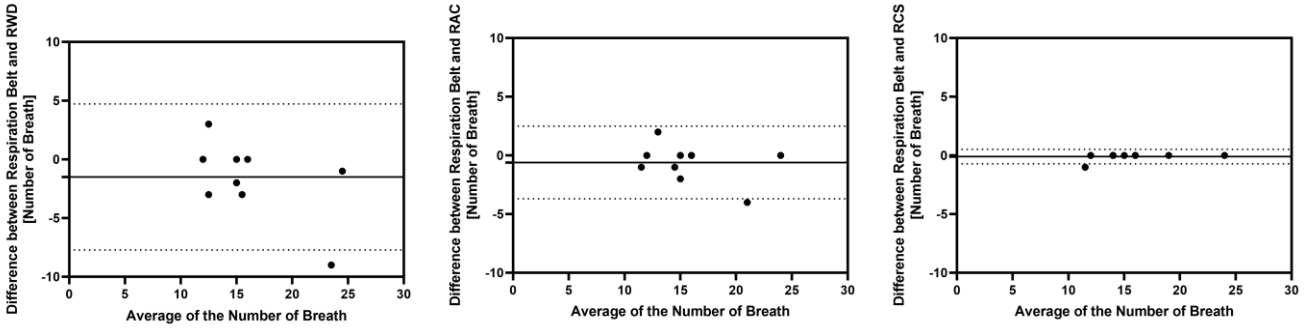


**FIGURE 9.** Bland-altman plots evaluating systematic bias of different methods against ground truth (respiration belt).

coefficients for the RAC method were 0.58, 0.62, and 0.57, respectively, for the corresponding cases. Conversely, the RCS method, which combined the DBSCAN clustering with the cluster selection algorithm, exhibited substantial performance improvements. This is evident from the achieved mean Pearson correlation coefficients of 0.84, 0.75, and 0.84, respectively, for the aforementioned cases. These results underscore a significant enhancement in both accuracy and reliability.

When comparing the method without clustering and the method using clustering but without the cluster selection method, the means of the Pearson correlation coefficient

were 0.61 and 0.76, respectively, showing that the differences were not statistically significant. This means that the clustering method partially clusters not only the pressure changes related to breathing, but also those not related to breathing. It was found that only the respiration-related pressure changes were reselected through the cluster selection method. Therefore, the respiration-related region was well segmented when using the cluster selection method. It was also found that the method without clustering and the method using all clusters were affected by the input volume, while they were least affected by the various input volumes. This shows that the cluster-selection method allows us to estimate the respiration waveform that is most similar to that of the respiration belt.

Recent research using pressure sensors to measure the respiration activity was mainly focused on extracting a representative respiratory frequency from the signals of the sensor or on selecting a sensor from pressure sensor arrays. The method of selecting a sensor that best represents breathing is not appropriate when the breathing pattern changes or the region to which pressure is applied by breathing changes over time. In this study, instead of selecting a sensor, clustering method combined with cluster selection method was applied to select the cluster that best represents the respiration pattern. By using this method, it was feasible to measure respiration by dynamically segmenting the area where pressure is generated by respiration.

In calculating the respiration waveform in this paper, three time-intervals (1-, 15-, and 30-sample intervals) were compared to calculate the pressure difference. Because the data of the mattress sensor was obtained from 14 to 15 Hz, the 15-sample and 30-sample intervals corresponded to about 1 second and about 2 seconds, respectively. Given that the normal breathing of a person is 12 to 20 times per minute, one breathing cycle is equivalent to 3 to 5 seconds. Therefore, we compared 30-sample and 15-sample intervals (2 seconds and 1 second corresponding to a half period and a quarter period of shallow breathing). We found that the respiration waveforms calculated were the most similar to the respiration waveforms of the respiration belt at 30-sample intervals, which is the half period of a respiratory cycle.

For the cluster selection, the respiration signal with the highest peak in the frequency band between 0.1 and 1 Hz was selected. These frequency bands were selected considering that the normal breathing frequency is within 0.2 to 0.7 [32]. Frequencies higher than 1 Hz in the frequency band were regarded as abnormal because it is too fast for normal breathing, and frequencies below 0.1 Hz were considered as baseline noise.

The limitation of this study was that only two healthy men were participated in the experiment to show the feasibility of the mattress sensor. However, since various groups of people did not participate in the experiment, only respiration signal and respiratory rate accuracy according to various input volumes were provided. The verifications for various groups of people and applications are in the scope of our future work. The use of a mattress sensor does have limitations. If the blanket or mattress is too thick, it may impede the proper transmission of pressure from the chest during respiration, rendering it impossible to measure breathing accurately using this sensor. Additionally, the pressure measurement area of the mattress sensor is limited to $24 \times 24\text{cm}^2$. If pressure transmission occurs outside this area, it can result in decreased measurement accuracy. Furthermore, the pressure measurement range is limited to 0 to 100 kg. Individuals who exceed this weight limit may also pose challenges for accurate measurements using the sensor. Additionally, as the sensor is wired and connected to a computer, it may cause inconvenience to the user. Developing a wireless version of the sensor would enhance usability and provide a better user experience.

## V. CONCLUSION

In this paper, a clustering method combined with a cluster selection algorithm, was proposed to show that human respiration can be estimated using a mattress sensor. The proposed method was compared with a method of calculation of the respiration waveform without clustering and a method that used clustering without using the cluster selection method. The mean Pearson correlation coefficients calculated were 0.88, 0.76, and 0.61, respectively, showing that the respiration waveforms calculated by the proposed method were most similar to those using the respiration belt. The difference in the correlation coefficients were statistically significant ($p < 0.001$). In addition, high correlation values were calculated for the various input volumes without being affected by the change in input volume, and the respiration rate generated by the proposed method also showed the greatest accuracy. Therefore, it was found that the proposed method was a good choice to estimate human respiration rates accurately using a mattress sensor.

## REFERENCES

[1] F. Scopesi, M. G. Calevo, P. Rolfe, C. Arioni, C. Traggiai, F. M. Risso, and G. Serra, "Volume targeted ventilation (volume guarantee) in the weaning phase of premature newborn infants," *Pediatric Pulmonol.*, vol. 42, no. 10, pp. 864–870, Oct. 2007, doi: 10.1002/ppul.20667.

[2] M. Chu, T. Nguyen, V. Pandey, Y. Zhou, H. N. Pham, R. Bar-Yoseph, S. Radom-Aizik, R. Jain, D. M. Cooper, and M. Khine, "Respiration rate and volume measurements using wearable strain sensors," *NPJ Digit. Med.*, vol. 2, no. 1, p. 8, Feb. 2019, doi: 10.1038/s41746-019-0083-3.

[3] F.-T. Wang, H.-L. Chan, C.-L. Wang, H.-M. Jian, and S.-H. Lin, "Instantaneous respiratory estimation from thoracic impedance by empirical mode decomposition," *Sensors*, vol. 15, no. 7, pp. 16372–16387, Jul. 2015, doi: 10.3390/s150716372.

[4] N. Molinaro, C. Massaroni, D. Lo Presti, P. Saccomandi, G. Di Tomaso, L. Zollo, P. Perego, G. Andreoni, and E. Schena, "Wearable textile based on silver plated knitted sensor for respiratory rate monitoring," in *Proc. 40th Annu. Int. Conf. IEEE Eng. Med. Biol. Soc. (EMBC)*, Jul. 2018, pp. 2865–2868, doi: 10.1109/EMBC.2018.8512958.

[5] M. Yu, J. Liou, S. Kuo, M. Lee, and Y. Hung, "Noncontact respiratory measurement of volume change using depth camera," in *Proc. Annu. Int. Conf. IEEE Eng. Med. Biol. Soc.*, Aug. 2012, pp. 2371–2374, doi: 10.1109/EMBC.2012.6346440.

[6] A. Kwasniewska, M. Szankin, J. Ruminski, and M. Kaczmarek, "Evaluating accuracy of respiratory rate estimation from super resolved thermal imagery," in *Proc. 41st Annu. Int. Conf. IEEE Eng. Med. Biol. Soc. (EMBC)*, Jul. 2019, pp. 2744–2747, doi: 10.1109/EMBC.2019.8857764.

[7] L. Scalise, N. Bernacchia, I. Ercoli, and P. Marchionni, "Heart rate measurement in neonatal patients using a webcamera," in *Proc. IEEE Int. Symp. Med. Meas. Appl.*, May 2012, pp. 1–4, doi: 10.1109/MeMeA.2012.6226654.
[8] Y. S. Lee, P. N. Pathirana, C. L. Steinfort, and T. Caelli, "Monitoring and analysis of respiratory patterns using microwave Doppler radar," *IEEE J. Transl. Eng. Health Med.*, vol. 2, 2014, Art. no. 1800912, doi: 10.1109/JTEHM.2014.2365776.
[9] J. Lee and S. K. Yoo, "Radar-based detection of respiration rate with adaptive harmonic quefrency selection," *Sensors*, vol. 20, no. 6, p. 1607, Mar. 2020.
[10] A. Czyżewski, B. Kostek, A. Kurowski, K. Narkiewicz, B. Graff, P. Odya, T. Śmiałkowski, and A. Sroczyński, "Algoritmically improved microwave radar monitors breathing more acurrate than sensorized belt," *Sci. Rep.*, vol. 12, no. 1, p. 14412, Aug. 2022, doi: 10.1038/s41598-022-18808-2.
[11] M. H. Jones, R. Goubran, and F. Knoefel, "Reliable respiratory rate estimation from a bed pressure array," in *Proc. Int. Conf. IEEE Eng. Med. Biol. Soc.*, Aug. 2006, pp. 6410–6413, doi: 10.1109/IEMBS.2006.260164.
[12] D. I. Townsend, M. Holtzman, R. Goubran, M. Frize, and F. Knoefel, "Measurement of torso movement with delay mapping using an unobtrusive pressure-sensor array," *IEEE Trans. Instrum. Meas.*, vol. 60, no. 5, pp. 1751–1760, May 2011, doi: 10.1109/TIM.2010.2092872.
[13] M. Holtzman, D. Townsend, R. Goubran, and F. Knoefel, "Breathing sensor selection during movement," in *Proc. Annu. Int. Conf. IEEE Eng. Med. Biol. Soc.*, Aug. 2011, pp. 381–384, doi: 10.1109/iembs.2011.6090123.
[14] J. M. Kortelainen, M. van Gils, and J. Pärkkä, "Multichannel bed pressure sensor for sleep monitoring," in *Proc. Comput. Cardiol.*, Sep. 2012, pp. 313–316.
[15] S. Nizami, A. Bekele, M. Hozayen, K. J. Greenwood, J. Harrold, and J. R. Green, "Measuring uncertainty during respiratory rate estimation using pressure-sensitive mats," *IEEE Trans. Instrum. Meas.*, vol. 67, no. 7, pp. 1535–1542, Jul. 2018, doi: 10.1109/TIM.2018.2805154.
[16] S. Nizami, A. Bekele, M. Hozayen, K. Greenwood, J. Harrold, and J. R. Green, "Comparing time and frequency domain estimation of neonatal respiratory rate using pressure-sensitive mats," in *Proc. IEEE Int. Symp. Med. Meas. Appl. (MeMeA)*, May 2017, pp. 239–244, doi: 10.1109/MeMeA.2017.7985882.
[17] X. Wu, V. Kumar, J. Ross Quinlan, J. Ghosh, Q. Yang, H. Motoda, G. J. McLachlan, A. Ng, B. Liu, P. S. Yu, Z.-H. Zhou, M. Steinbach, D. J. Hand, and D. Steinberg, "Top 10 algorithms in data mining," *Knowl. Inf. Syst.*, vol. 14, no. 1, pp. 1–37, Jan. 2008, doi: 10.1007/s10115-007-0114-2.
[18] J. MacQueen, "Some methods for classification and analysis of multivariate observations," in *Proc. 5th Berkeley Symp. Math. Statist. Probab.*, vol. 1. Berkeley, CA, USA: Univ. of California Press, 1967, pp. 281–297.
[19] L. AbdAllah and I. Shimshoni, "Mean shift clustering algorithm for data with missing values," in Data *Warehousing and Knowledge Discovery*. Cham, Switzerland: Springer, 2014, pp. 426–438.
[20] D. Demirović, "An implementation of the mean shift algorithm," *Image Process. Line*, vol. 9, pp. 251–268, Sep. 2019, doi: 10.5201/ipol.2019.255.
[21] L. Moraru, S. Moldovanu, L. T. Dimitrievici, N. Dey, A. S. Ashour, F. Shi, S. J. Fong, S. Khan, and A. Biswas, "Gaussian mixture model for texture characterization with application to brain DTI images," *J. Adv. Res.*, vol. 16, pp. 15–23, Mar. 2019, doi: 10.1016/j.jare.2019.01.001.
[22] T. M. Nguyen, "Gaussian mixture model based spatial information concept for image segmentation," Univ. Windsor, Windsor, ON, Canada, 2011.
[23] S. Sanjay-Gopal and T. J. Hebert, "Bayesian pixel classification using spatially variant finite mixtures and the generalized EM algorithm," *IEEE Trans. Image Process.*, vol. 7, no. 7, pp. 1014–1028, Jul. 1998, doi: 10.1109/83.701161.
[24] A. Moreira, M. Y. Santos, and S. Carneiro, "Density-based clustering algorithms–DBSCAN and SNN," Univ. Minho, Braga, Portugal, 2005, p. 18, vol. 1.
[25] M. Debnath, P. K. Tripathi, and R. Elmasri, "K-DBSCAN: Identifying spatial clusters with differing density levels," in *Proc. Int. Workshop Data Mining Ind. Appl. (DMIA)*, Sep. 2015, pp. 51–60, doi: 10.1109/DMIA.2015.14.
[26] *Micro Force Sensor*. Accessed: 2022. [Online]. Available: http://en.mspt.co.kr/rd/micro-force-sensor
[27] *Respiration Recording*, BIOPAC Syst., Goleta, CA, USA, 2023.
[28] *How the Lungs Work*. Accessed: 2022. [Online]. Available: https://www.nhlbi.nih.gov/health-topics/how-lungs-work
[29] K. Oh, C. S. Shin, J. Kim, and S. K. Yoo, "Level-set segmentation-based respiratory volume estimation using a depth camera," *IEEE J. Biomed. Health Informat.*, vol. 23, no. 4, pp. 1674–1682, Jul. 2019, doi: 10.1109/JBHI.2018.2870859.
[30] X. Xu, M. Ester, H.-P. Kriegel, and J. Sander, "A distribution-based clustering algorithm for mining in large spatial databases," in *Proc. 14th Int. Conf. Data Eng.*, Feb. 1998, pp. 324–331, doi: 10.1109/ICDE.1998.655795.
[31] F. Huang, Q. Zhu, J. Zhou, J. Tao, X. Zhou, D. Jin, X. Tan, and L. Wang, "Research on the parallelization of the DBSCAN clustering algorithm for spatial data mining based on the spark platform," *Remote Sens.*, vol. 9, no. 12, p. 1301, Dec. 2017.
[32] T. Taheri and A. Sant'Anna, "Non-invasive breathing rate detection using a very low power ultra-wide-band radar," in *Proc. IEEE Int. Conf. Bioinf. Biomed. (BIBM)*, Nov. 2014, pp. 78–83, doi: 10.1109/BIBM.2014.6999272.